RSC Advances

PAPER

View Article Online
View Journal | View Issue

Cite this: *RSC Adv.*, 2017, **7**, 43455

Magnetization of eugenol to fabricate magnetic-responsive emulsions for targeted delivery of caffeic acid phenethyl ester

Tao Wang,[abcd] Ren Wang,[abc] Zhengxing Chen *[abc] and Qixin Zhong*[d]

Fabrication of manipulative colloidal vehicles with appreciable stability under an eco-friendly, cross-linkage free environment has long been one of the major challenges in targeted delivery for curative, acoustic, and imaging purposes. A new targeted delivery system was developed in this paper based on magnetization of eugenol with magnetic Fe_3O_4 nanoparticles by simply evaporating water from the 3-phase system prior to a one-step coating of the oil using rice proteins to form core/shell structured composites. The droplets, examined as well-defined spheres with a mean hydrodynamic diameter of 204 nm, were metastable against long-term storage for up to 4 months, thermal treatment for up to 90 °C and UV (365 nm) radiation for up to 24 h. Furthermore, upon an external manipulation, the magnetic emulsions enhanced the anti-proliferation effects of encapsulated CAPE, an anti-cancer drug, on HCT-116 cells by over 20% compared to CAPE encapsulated in normal emulsions at dosages of 0.2 and 2 μg mL^{-1}. In principle, a wide variety of o/w emulsions can be magnetized using this approach. As a first step towards magnetic delivery, magnetization of oil may become a new targeted delivery strategy in the development of future site-specific diagnosis and treatment.

Received 24th July 2017
Accepted 3rd September 2017

DOI: 10.1039/c7ra08167g

rsc.li/rsc-advances

Introduction

Nanotechnology provides incredible opportunities for developing micro carriers encapsulating drugs,[1] nutraceuticals,[2] bioactives,[3] *etc.*, for their protective delivery pathways. Optimized drug delivery practices entail successful fabrication of biocompatible carriers and effective delivery of curative and bioactive compounds suffering from various drawbacks such as low solubility, poor absorption in the digestive tract, and low bioavailability, poor stability at the target sites.[4] Since vegetable proteins are among the biocompatible, biodegradable materials and are extensively explored as a potential *in vitro* drug carrier medium, a combination of such protein-based drug carriers and targeted delivery is therefore particularly appealing.[5] Superparamagnetic iron oxide nanoparticles (SPIONs) have their metabolic pathways in human blood with high biocompatibility and biodegradability.[6] The combination of SPIONs with protein-based carriers allows for the deposition and accumulation of drugs from outside the patient's body using suitable force fields in a highly site-specific fashion.

Despite pioneering efforts regarding carrier fabrication,[7] magnetization,[8] and targeted delivery,[9] the motive to improved formulations, strategies, and specialized approaches is still imperative and challenging. SPIONs anchoring is among the most critical steps towards magnetization of drug carriers. One sort of techniques is to incorporate SPIONs into protein shells through covalent binding between carboxyl groups (negative charge) and amino groups (positive charge). In a practical scenario, SPIONs are brought to reaction by surface modification[10] or by dissolving in cyclohexane,[11] chloroform[12] or dichloromethane,[13] and subsequent synthesis generally involves the usages of unwelcome cross-link agents like polyvinyl alcohol,[13] poly(allylamine hydrochloride), and sodium poly(styrene-4-sulfonate)[14] for desired grafting. However, these methods yielded microspheres with short storage life, low stability, and high toxicity.[11] Another technique for magnetization is by well suspending SPIONs in oil phase, followed by emulsification to form magnetic-responsive hybrid composites.[15] Due to a lack of affinity between oil and SPIONs, this approach is forwarded using solid oil as a disperse phase. The resultant carriers revealed no significant, extremely slow release of encapsulated drugs, thus, envisaged as of low practical interests for therapeutic purposes.

Suspensions of SPIONs in a liquid-oil phase without contributions from intermolecular linkages are intriguing with the aim of engineering a carrier filled with a magnetic, nontoxic

[a]State Key Laboratory of Food Science and Technology, Jiangnan University, Wuxi 214122, People's Republic of China. E-mail: zxchen_2008@126.com
[b]National Engineering Laboratory for Cereal Fermentation Technology, Jiangnan University, Wuxi 214122, People's Republic of China
[c]School of Food Science and Technology, Jiangnan University, Wuxi 214122, People's Republic of China
[d]Department of Food Science and Technology, University of Tennessee, Knoxville, TN, 37996-4539, USA. E-mail: qzhong@utk.edu

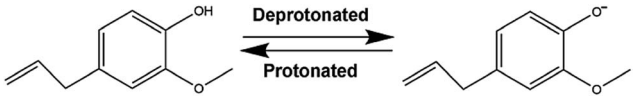

Scheme 1 Chemical structure of native and deprotonated eugenol.

core. Eugenol is slightly soluble in water with a solubility of 2.46 mg mL^{-1} (ref. 16) and a pK_a of 10.19 (ref. 17) at 25 °C. By carrying a hydroxyl on its phenolic ring, eugenol can be deprotonated or protonated following the chemical environment of solutions, as showed in Scheme 1. On the other hand, solid oxide particles immersed in aqueous electrolyte solutions can develop surface electrical charges by adsorption or desorption of potential-determining ions like OH^- or H^+ (ref. 18). Some reports confirmed a negatively charged state of SPIONs under acidic conditions.[19,20] Therefore, it is a comparatively simple step for charge transfer from eugenol to water and, subsequently, from water to SPIONs. We therefore hypothesized that the positively charged SPIONs not only create self-repulsion but supply counterions for deprotonated eugenol.

Earlier studies from our group have shown that by adjusting emulsion pH from 9.0 to neutral-adjacent range, modified rice proteins (MRPs) can preferentially precipitate around soybean oil droplets, and resulted emulsions demonstrated well-defined core/shell structures at a final pH of 6.6 (ref. 21). Here, we present a new, robust method for magnetization of eugenol, followed by deposition of rice proteins to fabricate magnetized-core protein-sell composites for targeted delivery. The strategy was based on mixing aqueous SPIONs solutions with eugenol (oil) under mild heat (80 °C) and extensive evaporation of moistures from the three-phase system. Specifically, the first objective was to characterize SPIONs suspensions from a mechanistic perspective. The secondary objective was to investigate the characteristics of emulsions, including morphologies, magnetism, and stabilities. The third objective was to study targeted delivery properties of the magnetic emulsions by investigating the viabilities of HCT-116 cells treated with caffeic acid phenethyl ester (CAPE) encapsulated in emulsions with or without SPIONs loading under external magnetic field.

Experimental section

Materials

Rice protein isolate powder containing 90.14 wt% protein, determined by the Kjeldahl method,[22] was purchased from Jinnong Biotechnology Ltd. (Yichun, Jiangxi, China). Eugenol, $FeSO_4 \cdot 7H_2O$, $FeCl_3 \cdot 6H_2O$, caffeic acid phenethyl ester (CAPE), dimethyl sulfoxide (DMSO), and fetal bovine serum (FBS) were purchased from Sigma-Aldrich Corp. (St. Louis, MO, USA). Human colon cancer cell line HCT-116 were purchased from American Type Culture Collection (Manassas, VA, USA) and were cultured in McCoy's media (Mediatech, Herdon, VA, USA). All other chemicals were of an analytical grade and were used without further purification.

Preparation of MRPs

MRPs were prepared according to our previous study.[23] In brief, rice proteins were suspended in distilled water (1 : 30, w/v) containing 0.03 M NaOH, incubated overnight at −20 °C, and directly milled using an impact mill (model XFB-500, Zhongcheng Mechanical Co., Changsha, China). The milled suspension after warming to room temperature (25 °C) was adjusted to pH 7.0 and centrifuged at 7000*g* for 10 min. The supernatant was transferred and desalted by dialysis against distilled water using a Fisherbrand membrane (Thermo Scientific Co., Marietta, OH, USA) with a molecular-weight-cut-off (MWCO) of 1000 Da, followed by freeze-drying to prepare lyophilized powder as the MRPs.

Synthesis of magnetic Fe_3O_4 nanoparticles (SPIONs)

The Fe_3O_4 SPIONs were prepared through an improved chemical co-precipitation method.[20] Briefly, a mixture of $FeCl_3 \cdot 6H_2O$ and $FeSO_4 \cdot 7H_2O$ was dissolved in water by a molar ratio of 2 : 1 (100 mL degassed by bubbling N_2 prior to use) and heated to 80 °C under N_2 protection along with vigorously agitation under mechanical stirring. Meanwhile, aqueous $NH_3 \cdot H_2O$ (25%, 10 mL) was added by a syringe for maintaining the pH approximately at 10 and heated for an additional 30 min. The reaction mixture was cooled to room temperature under continuous nitrogen protection. The supernatant was while the SPIONs were kept in the reaction flask using a magnet, and then the SPIONs were rinsed with distilled water for dozens of times. Finally, the SPIONs were air dried for further analysis.

Preparation of SPIONs suspensions in eugenol

SPIONs were mixed with distilled water by a solid : liquid ratio of 1 : 20. 10 mL of eugenol was added into equal volume of aqueous SPIONs under vigorous mechanic stirring accompanied by mild heating at 80 °C to allow evaporation of moisture. After 24 h stirring, aqueous water was fully removed, and the SPIONs suspensions were allowed to cool at room temperature. The resulting suspensions were centrifuged at 5000*g* to remove unstable Fe_3O_4 aggregates.

Preparation of magnetic emulsions (Mag-emulsions)

Stock aqueous solutions were prepared with 1% w/v MRPs in distilled water and adjusted to pH 9.0 with 0.1 M NaOH. SPIONs loaded eugenol was mixed with the protein stock solution at a volume ratio of 3 : 100 using a mixer (model T18BS25, IKA, Wilmington, NC, USA) at gear 5 for 60 s to obtain a pre-emulsion that was constantly stirred to suspend oil drops. To coat oil droplets with MRPs, 0.01 M HCl was drop-wise added to the pre-emulsion at room temperature until it reached a final pH of 6.6. The resulted emulsions were used for characterization as magnetic emulsions (Mag-emulsions). For comparison, pure eugenol was also emulsified and coated with MRPs at the same condition mentioned above to prepare a control (Con-emulsions).

Characterization of SPIONs suspension

Turbidity measurements. During the preparation of SPIONs suspensions, 100 μL of the oil phase was pipetted into a testing tube, and diluted by 60 times with eugenol. After centrifuged at 4000*g* for 10 min, the mixture was measured for absorbance at 600 nm (ref. 24) using eugenol as blank.

pH measurements. 50 mL of distilled water was stirred with incrementing fractions of eugenol, followed by measurements of pHs using a Mettler-Toledo-51302910 pH meter (Columbus, OH, USA) at room temperature.

UV-vis spectrum. Eugenol was treated at an equal condition to preparation of SPIONs suspensions but without SPIONs addition. After proper dilutions with ethanol, the absorbance spectra of untreated eugenol, heated eugenol and SPIONs suspensions were acquired from 200 to 600 nm using an Evolution 201 UV-vis spectrophotometer (Thermo Scientific, Waltham, MA).

Fourier transform infrared spectroscopy (FTIR). FTIR experiments were carried out using a Nicolet iS10 FTIR spectrometer (ThermoFisher Scientific Co., Marietta, OH, USA). About 2 μL of oil were mixed with KBr, followed by grinding and pressing into a pellet. The absorbance intensities were measured at a 2 cm^{-1} resolution in the wavenumber range of 4000–400 cm^{-1}.

Microscopic observations

Atomic force microscopy (AFM). The fresh Mag-emulsions (SPIONs suspensions) were diluted by 250 times with distilled water (ethanol), followed by spread on a freshly-cleaved mica sheet. AMF images were collected at tapping mode using a Nano-probe cantilever tip (BrukerNanoprobe, Camarillo, CA, USA) at a frequency from 50 to 100 kHz on a Multimode VIII microscope (Bruker Corporation, Billerica, MA, USA). Images were analyzed using the AFM instrument software (Nanoscope Analysis version 1.50, Bruker Corporation, Billerica, MA, USA).

3-D confocal imagery. MRPs and oil were stained with 100 μM nile blue and 100 μM nile red, respectively, before preparing Mag-emulsions as above. 3D imagery was acquired with a TCS SP2 LSCM confocal microscope (Leica, Wetzlar, Germany). A full three-dimensional model is reconstructed by assembling ten layers.

Scanning transmission electron microscopy (STEM). 10 μL of fresh emulsions was drop-cast on a holey carbon grid that was then kept flat for 1 min to allow droplet attachment. The drop was then dried with filter paper, and STEM images were obtained using a Zeiss Auriga 60 dual beam instrument (Carl Zeiss Microscopy, Oberkochen, Germany) operated at an accelerating voltage of 30 keV.

Size and zeta-potential

Droplet size and distributions and zeta-potential were determined at room temperature. Emulsions were diluted by 100 times using distilled water before testing on a Malvern Nano ZS (Malvern Instrument Ltd, Worcestershire, UK).

Superconductive quantum interference device (SQUID)

A magnetometer from Quantum Design MPMS5XL was used to perform magnetization measurements. About 3 mg of SPIONs or spray-dried Mag-emulsions were inserted into the sample holder. Magnetization curves were measured from −3000 to 3000 Oe at 5 K upon zero field cooling (ZFC). The remnant magnetization value of samples was divided by the weight of the analyzed powder (emu g^{-1}). Subsequently, the remnant magnetization per gram of spray-dried Mag-emulsions divided by that of SPIONs gave the average amount of magnetic material inside a droplet.

Interfacial tension

The surface tension between eugenol and water (γ_{e-w}) and eugenol and MRP stock solution (γ_{e-m}) was tested on a Cahn DCA 322 analyzer (Thermo Scientific Co., Marietta, OH, USA) using a Du Nouy ring as the probe. 25 mL eugenol and an identical volume of water/MRP solutions in a 100 mL beaker were used for each test. The platinum–iridium Du Nouy ring was immersed in the heavier phase under the interface. The force required to pull the ring from heavier to the lighter phase until interface breakdown was monitored in the process to calculate the interfacial tension (γ), which is corrected by a correction factor φ summarized by Zuidema and Waters:[25]

$$\gamma' = \frac{F_{\max} g}{4\pi R} \tag{1}$$

$$\varphi = 0.725 + \sqrt{\frac{1.452 F_{\max}}{4\pi^2 R^2 (\rho_1 - \rho_2)} + 0.04534 - \frac{1.679}{R/r}} \tag{2}$$

$$\gamma = \varphi \gamma' \tag{3}$$

where $F_{\max}$ is the maximum pulling force (mN) during the testing, g is the acceleration of gravity, R and r are the radius (cm) of Du Nouy ring and the wire of the ring, respectively, given by the manufacture, ρ_1 and ρ_2 are the densities (g mL^{-1}) of the heavier and lighter phase, respectively.

Emulsion stability

Long-term storage. Fresh Mag-emulsions were seal kept in an air oven with controlled temperature of 30 °C for up to 4 months, and samples collected from the first-month storage were analyzed.

Thermal treatment. Fresh Mag-emulsions were heated at 60–90 °C for 1 h in a water bath, and then immediately cooled in a 25 °C water bath before following analyses.

UV radiation. Effects of UV radiation on physical stability of magnetic emulsions were studied at 254 (UVc), 302 (UVb) and 365 nm (UVa) for up to 24 h at room temperature using a XX-15 series UV system equipped with 15 W UV lamps (UVP, LLC, Upland, CA). Samples were contained in transparent glass vials and were radiated under the lamp at an identical distance of 15 cm. After radiation, samples were stored in dark at room temperature for further tests.

After each treatment, the hydrodynamic diameter (D_h) and zeta-potential of Mag-emulsions were analyzed and used as indicators of stability.

Cell proliferation assays

CAPE was separately dissolved in SPIONs suspensions or eugenol at a final concentration of 20 mg mL^{-1}, then emulsified by MRPs as above mentioned. Fresh Mag-emulsions or Con-emulsions with CAPE loading were properly diluted with distilled water to obtain working solutions with a CAPE concentration of 0.8 mg mL^{-1}. For comparison purposes, a CAPE solution (0.8 mg mL^{-1}) dissolved in DMSO was also prepared.

Cell proliferation was evaluated by using the method of Pan *et al.* with slight modifications.[26] Human colon cancer cell line HCT-116 cells were cultured in a media supplemented with 10% FBS, 100 unit per mL penicillin and 100 mg mL^{-1} streptomycin under a humidified atmosphere with 5% CO_2 at 37 °C. The anti-cancer activity of CAPE was tested using CellTiter 96 Aqueous One Solution Cell Proliferation Assay (Promega Corp., Madison, WI, USA). Briefly, HCT-116 cells were seeded in 96-well micro-titer plates at a density of 5000 cells per well in a final volume of 100 μL of media, underneath was a magnet to generate manipulation field. The cells were then treated with 0.2, 2 and 20 μg mL^{-1} of free (dissolved in DMSO) or encapsulated CAPE diluted from the working solutions in the cell media, followed by incubation for another 24 h under the above conditions. Positive controls were cells cultured in the media treated with CAPE-free DMSO or CAPE-free emulsions at the same concentrations as the CAPE-loaded counterparts, and negative control was the pure culture media. After 48 h treatment, 20 μL of CellTiter 96 Aqueous One Solution (Promega, WI, USA) was added to each well and then incubated for 1 h at 37 °C. The absorbance at 490 nm was measured with a microplate reader (Bio-Tek Instruments, Winooski, VT, USA). Normalized cell viability (V_N) was expressed using eqn (4):

$$V_N = \frac{A_{treated} - A_{Nc}}{A_{Pc} - A_{Nc}} \times 100\% \quad (4)$$

where $A_{treated}$ is the absorbance of CAPE-dosed cells, A_{Pc} is the absorbance of positive control, and A_{Nc} is the absorbance of negative control. The mean and standard deviation from at least four-well replicates were calculated.

Statistical analysis

The experiments were performed in triplicate, and values were expressed as mean ± standard deviation (SD). Analysis of variance was evaluated using the Duncan's multiple range test.

Results and discussion

Characterization of SPIONs suspensions

To maximize the accommodation of magnetic responsiveness on a carrier would statistically require increasing magnetic components. As such an increase is not possible under the constraints of limited reaction sites on coated structures, we instead chose incorporating SPIONs into an oil reservoir. The protocol was based on deprotonation of eugenol when brought to contact with water, followed by protonation of SPIONs by absorption of H^+, thus incorporating them into oil phase driven by electrostatic attraction (Fig. 1a). As showed by Fig. 1b, the turbidity in oil phase was enhanced by mixing eugenol and aqueous SPIONs along with elapsing time until peaked at 24 h. Further heating caused desorption of H^+ from SPIONs and again reduced the turbidity of eugenol. By contrast, simply mixing air-dried SPIONs in eugenol evidenced negligible incorporation. Considering that the pH of distilled water was systematically lowered by addition and stirring of eugenol until reached a final value of 3.05 (Fig. 1c), the comparison addressed an important role played by water that delivered H^+ from eugenol to SPIONs. After full evaporation of moisture, SPIONs and eugenol were oppositely charged, and the electrostatic interaction may be responsible for the colloidal stability of the suspensions which could be stable for over three months without visible sedimentation (data no shown).

The interaction stabilizing SPIONs was further confirmed by FTIR as being a non-covalent bridging between Fe_3O_4 and eugenol (Fig. 1d). The UV spectra indicated the same results, where the identical spectra among eugenol, heated eugenol, and SPIONs–eugenol suspensions evidenced the same nature of eugenol (Fig. 1e). AFM observations showed spherical particles

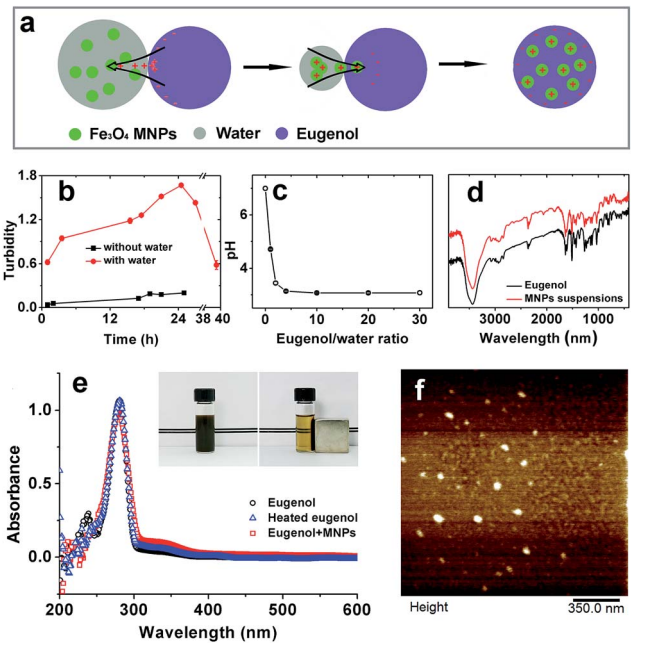

Fig. 1 Characterization of SPIONs suspensions. (a) Schematic illustration of the formation of stable SPIONs suspensions. Eugenol was deprotonated in contact with water, and the protons charged the SPIONs, which in turn stabilized the SPIONs in eugenol by electrostatic attraction when moisture was evaporated from the system. (b) Turbidity changes during mixing SPIONs with eugenol at 80 °C. (c) pH changes in water with incrementing addition of eugenol. (d) FTIR spectra of eugenol and SPIONs suspensions. (e) UV-vis spectra of eugenol, heated eugenol and SPIONs suspensions; the inset illustrated the collection of SPIONs from eugenol using a magnet. (f) AFM image of SPIONs particles.

of SPIONs with an average diameter of 20 nm (Fig. 1f), and the particles can be recycled under an external magnet field (inset of Fig. 1e).

Morphologies and structures of Mag-emulsions

From AFM topographical scans in a three-dimensional mode, it is possible to observe that the SPIONs loaded carriers were of well-defined spherical shapes and presented smooth surface (Fig. 2a), characterized by a mean diameter of 208 ± 40 nm, calculated *via* software analysis. The carrier structures can be distinguished by respectively scanning of fluorophore-stained components. Since CLSM is an optical instrument of relatively low resolution, only composite carriers larger than 1 μm were well resolved whereas smaller ones, especially those observed in AFM, were distorted or even invisible. Nevertheless, the observations showed that the carriers had obvious core/shell structures with a large size distribution resulted from heterogeneous nature of high speed emulsification (Fig. 2b). Experimental results from STEM illustrated compositional differences between emulsions without (control) or with SPIONs loading. As showed by representative STEM images, a droplet from Con-emulsions was evenly transmitted by electrons (Fig. 2c), whereas SPIONs loaded sample was decorated with dark spots (Fig. 2d) with a mean diameter similar to that observed by AFM, signifying the existence of SPIONs. Of note that both droplets in STEM showed deformed structures, which was probably due to the quick evaporation of eugenol under vacuum observations resulted from a high saturated vapor pressure (0.0221 mm Hg at 25 °C) of the oil model. The above microscopic observations collectively indicated that the carriers were composed of materials characterized by oil-core protein-shell structures with SPIONs embedded inside the lipid core, therefore suggesting successful magnetization of lipid–protein carriers.

Size and distributions

Both Con- and Mag-emulsions showed similar broad distributions in a bimodal pattern, with the majority sized between 100–900 nm. The peaks with bigger structures may be assigned to oil droplets with protein shells because the preparation process did not use high shear deformation, while the smaller ones may be assigned to protein-only particles. The polydispersibility index (PDI) calculated from the experiment was up to 0.49 and 0.43 for Con-emulsions and Mag-emulsions, respectively. The results agreed well with large SD in size calculations from AFM and wide size range in CLSM observations. However, droplet size was increased by up to 100 nm when SPIONs were encapsulated, compared to Con-emulsions. By deprotonation of hydroxyl and binding with SPIONs, eugenol may have been partially deprived

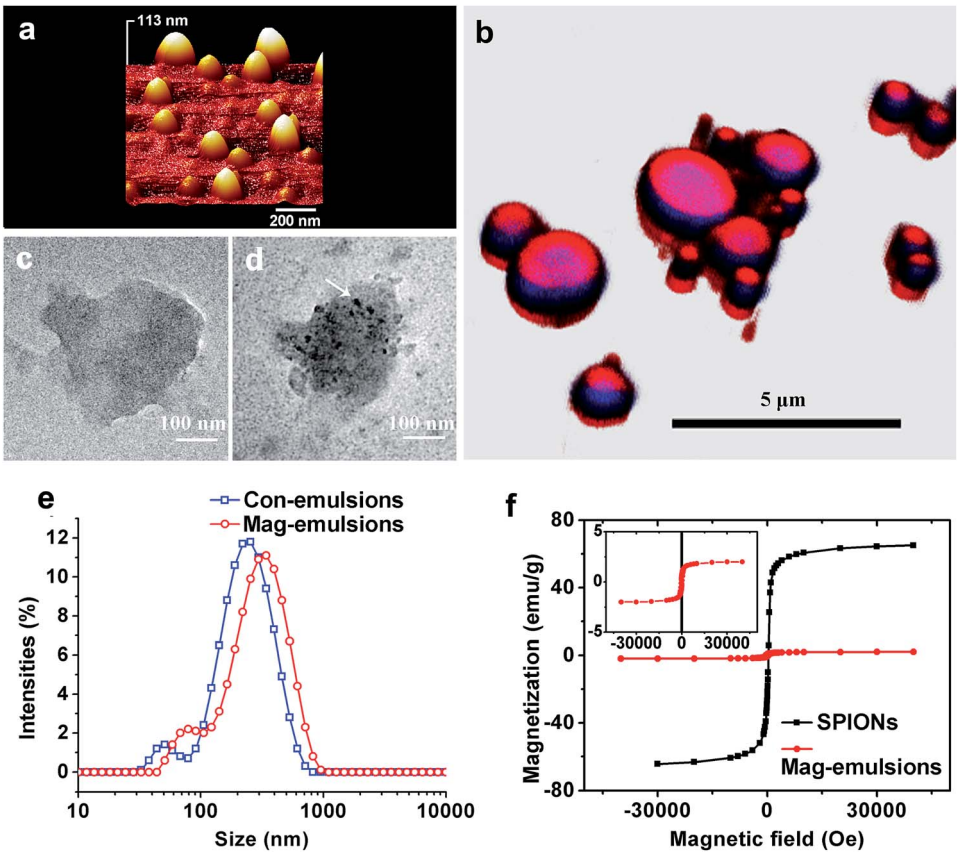

Fig. 2 Characterization of Mag-emulsions. (a) AFM image of Mag-emulsions in a 3-D mode. (b) CLSM image of Mag-emulsions; eugenol and MRPs were stained with nile red and nile blue, respectively. (c) STEM image of Con-emulsions. (d) STEM image of Mag-emulsions. (e) Size distributions of fresh emulsions. (f) Magnetic measurement of air-dried SPIONs and spray-dried Mag-emulsions.

of miscibility with water and hence, increasing the oil–water interfacial tension during emulsification. The capillary forces maximizing the oil surface area was therefore augmented, and so was the droplet size. Moreover, the increased size for protein-only particles was probably due to aggregation of smaller particles induced by eugenol.[27]

Filippidi and co-authors practiced a protocol similar to our study by lowering the alcohol content so that zein became precipitated on oil droplets, and a large PDI was also observed but a mean diameter of 30–40 μm was reported.[28] Apart from the differences in protein structures, the amphiphilic nature of eugenol played a significant role in reducing the droplet size,[29] again because of the ability to reduce oil–water interfacial tension. Of note that blood circulation of particles with size greater than 10–15 micrometers could jeopardize the capillaries thanks to infarction or blockage, leading to ischemia or oxygen deprivation and possible tissue death.[30]

Magnetization measurements

The hysteresis curves of pristine SPIONs and spray-dried Mag-emulsions were similar (Fig. 3b), thus indicating analogous magnetic properties between the two materials. The saturation magnetization at 5 K was 65 emu g^{-1} for SPIONs, while 2 emu g^{-1} for the carriers. Further considering that the magnetic moment of SPIONs should be identical with or without encapsulation, we can conclude that the percentage of SPIONs in the dried emulsions is about 3.1 wt%. The results were comparable to magnetic solid–lipid particles emulsified with Tween 80.[15] On the other hand, while SPIONs were homogeneously dispersed in the oil matrix (Fig. 2d) and retained superparamagnetic behavior (Fig. 2f) after the encapsulation process, the carriers presented the absence of magnetic dipoles and attractive interactions among oil droplets (Fig. 2a) that would cause embolism during the intravenous administration.[13]

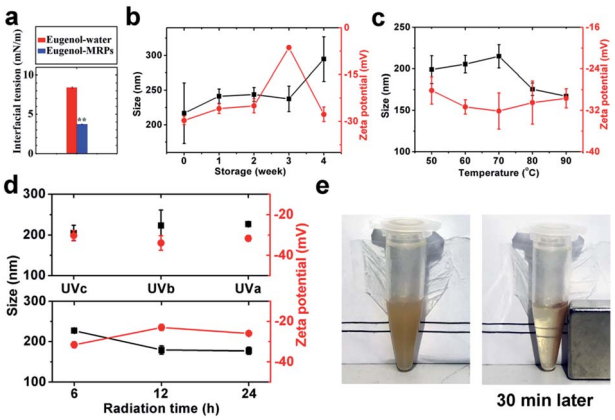

Fig. 3 Characterization of emulsion stabilities. (a) Eugenol–water interfacial tension with or without MRPs addition; double-asterisk indicates very significant difference ($p < 0.01$) from the control. (b) Hydrodynamic diameter (D_h, black line with square) and zeta-potential (red line with circle) changes along with long-term storage. (c) D_h (black line with square) and zeta-potential (red line with circle) changes along with temperature variations. (d) D_h (black line with square) and zeta-potential (red line with circle) changes under 6 h radiation using different UV lamps (top), and under UVa radiation over different durations (bottom). (e) Collection of Mag-emulsions using a magnet.

Emulsion stability

Protein emulsions were believed to be unconditionally instable due to the large interfacial energy moving proteins away from the interface,[31] leading to phase separation, which is detrimental to their applications in the food, cosmetic, and pharmaceutical industries. Ostwald ripening and coalescence are the two major factors governing the sedimentation and creaming of oil droplets, following linear and exponential growth of droplet size, respectively.[32] The former destabilization relies on the transport of oil to form large droplets at the expense of small ones, while the latter depends on the thinning and disruption of the liquid film that covers the droplets.[33,34]

MRPs was found to effectively reduce the interfacial tension between eugenol and water (Fig. 3a). This on one hand confirmed our former hypothesis about the formation of nanoscale sized droplets; on the other hand, accounted for the thermodynamic stability of the emulsions during 4 week storage (Fig. 3b). Apart from reduced interfacial tension, the competition between Laplace pressure and osmosis pressure can effectively resist Ostwald ripening and coalescence due to considerable water solubility of eugenol.[35] However, an appreciable decrease in surface charge occurred at 3rd week, followed by a relatively sharp increase in hydrodynamic diameter (D_h) at 4th week. Upon long-term storage, approaching droplets aggregate and expel water from the hydration layer,[36] burying charged groups and increasing D_h at 4th week. Interestingly, the droplets became charged again at 4th week, a plausible assumption is that aggregation was accompanied by osmosis of eugenol among droplets and the released eugenol in turn realigned the protein structures. In addition, the aggregated structure has a lower free energy than the structures in the native state ensemble thus making the folded state metastable.[37] The emulsions can be stable for another 3 months without visible sedimentation or creaming.

Thermal treatment can cause aggregation of protein-emulsified emulsions through exposed hydrophobic patches on the denatured proteins.[38] Being heated at temperatures from 60 to up to 90 °C, the emulsions maintained considerable colloidal stabilities without significant changes in zeta-potential (*ca.* −30 mV), assigned to excellent thermal stability of MRPs.[39] Then the progressive decrease of D_h from 70 to 90 °C suggested shrinkages of droplets due to release of eugenol.

When radiated by UV, proteins and other macromolecule can generate hydrogen peroxide and superoxide, oxidizing thiols to form disulfide bonds and leading to droplet aggregation.[40] As eugenol is a kind of free radical scavenger and suppresses oxidation of thiols on the side chains of proteins, both zeta-potential and D_h were not significantly changed during 6 h UV radiation among all tested wavelengths (top Fig. 3d). By increasing radiation time, however, UVa significantly lowered droplet surface charges but unexpectedly reduced D_h (bottom Fig. 3d). The reason may be that radiation partially removed hydration layer around droplet surface, which

accounts for a great part of the droplet size, by oxidizing and packing of protein coatings toward more hydrophobic structures.

Ostwald growth and coalescence are dominating in protein emulsions, only a limited kind of thermodynamic stability is attainable.[41] The above results demonstrated a high stability of the SPIONs loaded carriers, and the stability was reached by neither mechanical agitation nor addition of any surfactants as stabilizers. Nevertheless, a robust magnetic response was observed and could readily be used to manipulate and collect the carriers with an external magnetic field (Fig. 3e).

Improved bioavailability of encapsulated bioactives

CAPE is a kind of plant phenolic compounds suppressing the expression of β-catenin and reducing tumors in APC Min mice.[42] *In vitro* anti-cancer effect of CAPE is illustrated in Fig. 4. By dosed in culture medium, CAPE, either pre-dissolved in DMSO or encapsulated in emulsions, suppressed the viability of HCT-116 cells in a dose-dependent manner from 0.2 to 20 μg mL^{-1}. The cells were mostly or fully killed at a dosage of 20 μg mL^{-1} in all administrations, confirming that CAPE is effective anti-proliferation medicine. Carrier materials have the potential of improving cellular uptake of encapsulated bioactives.[43] CAPE encapsulated in Con-emulsions showed improved anti-proliferation activity when compared to CAPE pre-dissolved in DMSO, although the improvement was statistically insignificant ($p > 0.05$) at a dosage of 2 μg mL^{-1}.

The cell viability was further inhibited when CAPE was encapsulated in Mag-emulsions and manipulated under an external field. Compared to CAPE encapsulated in Con-emulsions, magnetically guided CAPE reduced the viability of HTC-116 cells by 21.4% ($p > 0.05$) and 23.2% ($p < 0.05$) at dosages of 0.2 and 2 μg mL^{-1}, respectively. Those values came to 30.3% ($p < 0.01$) and 33.3% ($p < 0.05$) as against CAPE pre-dissolved in DMSO at dosages of 0.2 and 2 μg mL^{-1}, respectively. The enhancement was correlated with improved membrane uptake of drug carriers and the accelerated release of drugs was proposed to result from the increased membrane fluidity before drug insertion.[43] The significantly enhanced anti-proliferation activity of manipulated CAPE further highlights the excellent potential of the present magnetization technology, *i.e.*, utilizing reactive oils as SPIONs reservoirs in synthesis of magnetic core/shell composites.

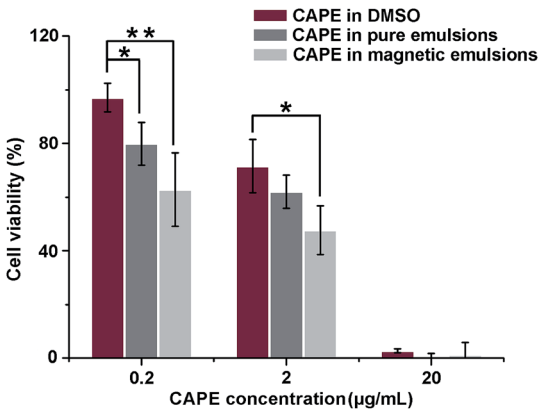

Fig. 4 Anti-proliferation activity of CAPE supplemented at 0.2, 2, and 20 mg mL^{-1}. A magnet was placed underneath the 96-well plate to apply magnetic field for the magnetic emulsions. Error bars are standard deviations ($n = 4$). The asterisks and double-asterisks above bars are significantly different ($p < 0.05$) and very significantly different ($p < 0.01$), respectively, from the same concentration of DMSO-dissolved CAPE.

Conclusions

By means of a straightforward evaporation in a double-solvent system, we successfully prepared magnetic responsive eugenol loaded with SPIONs. Using a one-step anti-solvation at a neutral-adjacent pH, eugenol-core MRPs-shell composites with magnetism were subsequently fabricated. The emulsion droplets were spherical, with a hydrodynamic diameter of around 204 nm, and can be readily controlled under an external field. Importantly, the Mag-emulsions were metastable against long-term storage, thermal treatment and UV radiation, which enabled their application in medical and pharmaceutical industries without the need of further addition of stabilizers. Also, using an external magnetic field as a governing tool, CAPE encapsulated in Mag-emulsions showed better anti-proliferation effects on HCT-116 cells than encapsulated in Con-emulsions or pre-dissolved in DMSO. The simple, robust, potent, and additive-free magnetization method simplifies magnetic delivery of oil-soluble components toward desired targets, which may become a new targeted delivery strategy in the development of future site-specific diagnosis and treatment.

Conflicts of interest

There are no conflicts to declare.

Acknowledgements

This work was supported by the National High Technology Research Development Program of China (863 Program) (No. 2013AA102204, 2013AA102206), National Natural Science Foundation of China (No. 31201381, 31471616 and 31371874) and Special Fund for Agro-Scientific Research in the Public Interest of China (No. 201303071). T. Wang would like to thank the scholarship provided by the China Scholarship Council. Q. Zhong would like to acknowledge the support from the University of Tennessee and the USDA National Institute of Food and Agriculture Hatch Project 223984.

References

1 S. Mura, J. Nicolas and P. Couvreur, Stimuli-responsive nanocarriers for drug delivery, *Nat. Mater.*, 2013, **12**, 991.
2 L. Chen and M. Subirade, Chitosan/β-lactoglobulin core–shell nanoparticles as nutraceutical carriers, *Biomaterials*, 2005, **26**, 6041.

3 L. Chen and M. Subirade, Alginate – whey protein granular microspheres as oral delivery vehicles for bioactive compounds, *Biomaterials*, 2006, **27**, 4646.
4 G. L. Amidon, H. Lennernäs, V. P. Shah and J. R. Crison, A theoretical basis for a biopharmaceutic drug classification: the correlation of in vitro drug product dissolution and in vivo bioavailability, *Pharm. Res.*, 1995, **12**, 413.
5 I. J. Joye and D. J. McClements, Biopolymer-based nanoparticles and microparticles: fabrication, characterization, and application, *Curr. Opin. Colloid Interface Sci.*, 2014, **19**, 417.
6 L. H. Reddy, J. L. Arias, J. Nicolas and P. Couvreur, Magnetic nanoparticles: design and characterization, toxicity and biocompatibility, pharmaceutical and biomedical applications, *Chem. Rev.*, 2012, **112**, 5818.
7 S. Lam, K. P. Velikov and O. D. Velev, Pickering stabilization of foams and emulsions with particles of biological origin, *Curr. Opin. Colloid Interface Sci.*, 2014, **19**, 490.
8 J. Dobson, Magnetic nanoparticles for drug delivery, *Drug Dev. Res.*, 2006, **67**, 55.
9 S. Ganta, H. Devalapally, A. Shahiwala and M. Amiji, A review of stimuli-responsive nanocarriers for drug and gene delivery, *J. Controlled Release*, 2008, **126**, 187.
10 D. Vlaskou, O. Mykhaylyk, F. Krötz, N. Hellwig, R. Renner, U. Schillinger, B. Gleich, A. Heidsieck, G. Schmitz and K. Hensel, Magnetic and acoustically active lipospheres for magnetically targeted nucleic acid delivery, *Adv. Funct. Mater.*, 2010, **20**, 3881.
11 W. Jiang, Z. Sun, F. Li, K. Chen, T. Liu, J. Liu, T. Zhou and R. Guo, A novel approach to preparing magnetic protein microspheres with core–shell structure, *J. Magn. Magn. Mater.*, 2011, **323**, 435.
12 H. Y. Koo, S. T. Chang, W. S. Choi, J.-H. Park, D.-Y. Kim and O. D. Velev, Emulsion-based synthesis of reversibly swellable, magnetic nanoparticle-embedded polymer microcapsules, *Chem. Mater.*, 2006, **18**, 3308.
13 E. Carenza, O. Jordan, P. Martínez-San Segundo, R. Jiřík, Z. Starčuk Jr, G. Borchard, A. Rosell and A. Roig, Encapsulation of VEGF 165 into magnetic PLGA nanocapsules for potential local delivery and bioactivity in human brain endothelial cells, *J. Mater. Chem. B*, 2015, **3**, 2538.
14 Y. Han, D. Radziuk, D. Shchukin and H. Moehwald, Sonochemical synthesis of magnetic protein container for targeted delivery, *Macromol. Rapid Commun.*, 2008, **29**, 1203.
15 A. Grillone, E. R. Riva, A. Mondini, C. Forte, L. Calucci, C. Innocenti, C. de Julian Fernandez, V. Cappello, M. Gemmi and S. Moscato, Active Targeting of Sorafenib: Preparation, Characterization, and In Vitro Testing of Drug-Loaded Magnetic Solid Lipid Nanoparticles, *Adv. Healthcare Mater.*, 2015, **4**, 1681.
16 S. H. Yalkowsky, Y. He and P. Jain, *Handbook of Aqueous Solubility Data*, CRC Press, 2016.
17 G. Kortüm, W. Vogel and K. Andrussow, Dissociation constants of organic acids in aqueous solution, *Pure Appl. Chem.*, 1960, **1**, 187.
18 R. Atkinson, A. Posner and J. P. Quirk, Adsorption of potential-determining ions at the ferric oxide–aqueous electrolyte interface, *J. Phys. Chem.*, 1967, **71**, 550.
19 A. Dong, S. Lan, J. Huang, T. Wang, T. Zhao, L. Xiao, W. Wang, X. Zheng, F. Liu and G. Gao, Modifying Fe_3O_4-functionalized nanoparticles with N-halamine and their magnetic/antibacterial properties, *ACS Appl. Mater. Interfaces*, 2011, **3**, 4228.
20 Z. Lu, Y. Qin, J. Fang, J. Sun, J. Li, F. Liu and W. Yang, Monodisperse magnetizable silica composite particles from heteroaggregate of carboxylic polystyrene latex and Fe_3O_4 nanoparticles, *Nanotechnology*, 2008, **19**, 055602.
21 T. Wang, R. Wang, Z. Chen and Q. Zhong, Coating oil droplets with rice proteins to control the release rate of encapsulated beta-carotene during in vitro digestion, *RSC Adv.*, 2016, **6**, 73627.
22 A. G. Gornall, C. J. Bardawill and M. M. David, Determination of serum proteins by means of the biuret reaction, *J. Biol. Chem.*, 1949, **177**, 751.
23 T. Wang, H. Zhang, L. Wang, R. Wang and Z. Chen, Mechanistic insights into solubilization of rice protein isolates by freeze–milling combined with alkali pretreatment, *Food Chem.*, 2015, **178**, 82.
24 M. Bachar, A. Mandelbaum, I. Portnaya, H. Perlstein, S. Even-Chen, Y. Barenholz and D. Danino, Development and characterization of a novel drug nanocarrier for oral delivery, based on self-assembled β-casein micelles, *J. Controlled Release*, 2012, **160**, 164.
25 H. Zuidema and G. Waters, Ring method for the determination of interfacial tension, *Ind. Eng. Chem.*, 1941, **13**, 312.
26 K. Pan, Y. Luo, Y. Gan, S. J. Baek and Q. Zhong, pH-driven encapsulation of curcumin in self-assembled casein nanoparticles for enhanced dispersibility and bioactivity, *Soft Matter*, 2014, **10**, 6820.
27 R. A. Frazier, A. Papadopoulou and R. J. Green, Isothermal titration calorimetry study of epicatechin binding to serum albumin, *J. Pharm. Biomed. Anal.*, 2006, **41**, 1602.
28 E. Filippidi, A. R. Patel, E. Bouwens, P. Voudouris and K. P. Velikov, All-Natural Oil-Filled Microcapsules from Water-Insoluble Proteins, *Adv. Funct. Mater.*, 2014, **24**, 5962.
29 Y. He, E. Heine, N. Keusgen, H. Keul and M. Möller, Synthesis and characterization of amphiphilic monodisperse compounds and poly(ethylene imine)s: influence of their microstructures on the antimicrobial properties, *Biomacromolecules*, 2013, **13**, 612.
30 N. P. Desai, P. Soon-Shiong, P. A. Sandford, M. W. Grinstaff and K. S. Suslick, Methods for in vivo delivery of substantially water insoluble pharmacologically active agents and compositions useful therefor, Utility Patent, US5439686, 1995.
31 S. Melle, M. Lask and G. G. Fuller, Pickering emulsions with controllable stability, *Langmuir*, 2015, **21**, 2158.
32 A. Kabalnov, A. Pertzov and E. Shchukin, Ostwald ripening in emulsions: I. Direct observations of Ostwald ripening in emulsions, *J. Colloid Interface Sci.*, 1987, **118**, 590.

33 N. L. Sitnikova, R. Sprik, G. Wegdam and E. Eiser, Spontaneously formed trans-anethol/water/alcohol emulsions: mechanism of formation and stability, *Langmuir*, 2005, **21**, 7083.
34 B. Binks, W. Cho, P. Fletcher and D. Petsev, Stability of oil-in-water emulsions in a low interfacial tension system, *Langmuir*, 2000, **16**, 1025.
35 A. Webster and M. Cates, Stabilization of emulsions by trapped species, *Langmuir*, 1998, **14**, 2068.
36 D. Thirumalai, G. Reddy and J. E. Straub, Role of water in protein aggregation and amyloid polymorphism, *Acc. Chem. Res.*, 2011, **45**, 83.
37 I. V. Baskakov, G. Legname, M. A. Baldwin, S. B. Prusiner and F. E. Cohen, Pathway complexity of prion protein assembly into amyloid, *J. Biol. Chem.*, 2002, **277**, 21140.
38 C. M. Bryant and D. J. McClements, Molecular basis of protein functionality with special consideration of cold-set gels derived from heat-denatured whey, *Trends Food Sci. Technol.*, 1998, **9**, 143.
39 T. Wang, F. Liu, R. Wang, L. Wang, H. Zhang and Z. Chen, Solubilization by freeze-milling of water-insoluble subunits in rice proteins, *Food Funct.*, 2015, **6**, 423.
40 C. Pourzand and R. M. Tyrrell, Apoptosis, the role of oxidative stress and the example of solar UV radiation, *Photochem. Photobiol.*, 1999, **70**, 380.
41 P. Taylor, Ostwald ripening in emulsions, *Adv. Colloid Interface Sci.*, 1998, **75**, 107.
42 N. N. Mahmoud, A. M. Carothers, D. Grunberger, R. T. Bilinski, M. R. Churchill, C. Martucci, H. L. Newmark and M. M. Bertagnolli, Plant phenolics decrease intestinal tumors in an animal model of familial adenomatous polyposis, *Carcinogenesis*, 2000, **21**, 921.
43 J. Wang, Y. Wang and W. Liang, Delivery of drugs to cell membranes by encapsulation in PEG–PE micelles, *J. Controlled Release*, 2012, **160**, 637.